Fermi National Accelerator Laboratory

TM-1422
2271.000

UPDATE ON THE TEVATRON MUON SHIELD

Anthony Malensek and Linda Stutte
Fermi National Accelerator Laboratory, Batavia, Illinois 60510

September 15, 1986

Operated by Universities Research Association Inc. under contract with the United States Department of Energy

TM-1422
2271.00

UPDATE ON THE TEVATRON MUON SHIELD

Anthony Malensek and Linda Stutte

September 15, 1986

INTRODUCTION

Early studies[1] of the original dirt neutrino berm called for the insertion of steel to harden the berm for Tevatron operation. These studies recommended a 1.8 m radius plug be buried downstream of enclosure NW4, with the goal of reducing muon backgrounds to 10 muons per square meter at the 15-ft. bubble chamber for 10^{13} 1 TeV protons on target. It was found that the length of the shield depended strongly upon the dE/dx formulation used in the calculations. Including atomic collisions and pair production only, the shield needed was calculated to be 250 m long. If energy loss due to bremsstrahlung was also included, the shield needed was calculated to be 150 m long.

In 1980, a 1.8 m radius plug was installed in the berm, extending approximately 150 m beyond enclosure NW4. Including packing fraction, about 130 m of steel was installed. Subsequent to this, approximately 30 m of dirt was removed at the end of the berm for Lab F. Original plans called for the insertion of additional material in enclosure NW4 to complete the shield.

In 1984, the NCI dichromatic train[2] was installed for an initial set of tests[3]. Along with these tests of train performance, measurements of muon rates at various depths in the berm were taken in order to check Monte Carlo predictions. Data were taken at a range of train momentum settings, and from a bare target. The results of those studies are presented here and compared to predictions. In 1985, the quadrupole triplet train[4] was installed for a wide band neutrino run. During this run, 5.5 m of 1.8 m diameter lead was installed in NW4 at the request of the experimenters to harden the shield. Data obtained during this triplet run under a variety of conditions are also presented, and compared to Monte Carlo predictions. Finally, these results are used to determine how much additional shielding is needed for higher energy operation.

MUON PENETRATION DATA

Figure 1 shows the location of monitors used in these studies. At Monitor Port 3 (NW5) a 1.65 m x 1.65 m ion chamber[5] was placed next to a group of 6 scintillation counters[6]. The counters (of size 0.5 m high by 1.5 m wide) were arranged in 3 back-to-back sets which formed coincidences and spanned roughly the same cross sectional area as the ion chamber. Locations NW6, NW8 upstream and NW8 downstream had only 4 scintillation counters, arranged in 2 back-to-back sets, spanning a vertical height of 1 m. The counter arrays were typically not placed exactly on beam center; the Monte Carlo calculations were adjusted for this effect. In the Wonder Building, the 1.5 m x 1.5 m T1 counters located in the muon spectrometer for E701[7] were used in coincidence. Primary intensity information was obtained from a SEM[8] located upstream of the production target in NW1. Intensity information from all of these monitors, as well as the currents in all train magnets were read out and recorded on magnetic tape each pulse. Slow spill (20 second duration) was used exclusively for these measurements. Intensities on target ranged from 5 x 10^{10} to 3 x 10^{12} protons per pulse.

Data were taken with the dichromatic train set from 200 to 600 GeV, with 800 GeV on target. In addition, the dichromatic production target was removed from the beam path, and 800 GeV primary protons were steered onto a one interaction length aluminum block ("the bare target") located downstream of the train, at the end of enclosure NW1.

Because data were taken at a range of intensities, a crude measure of systematic errors for the various points can be made. For the highest intensity points (200 and 300 GeV in NW5 and bare target in NW5 and NW6) measurement errors are probably in the 25-30% range. Lower intensity points are considerably lower than this. In addition, an overall scale uncertainty of 30-40% can not be ruled out.

The data taken with the dichromatic train and the bare target are shown in Figure 2, with error bars indicating the estimated point to point systematic errors. No reliable data was obtainable from the scintillators located in NW5 at a setting of 200 GeV. Instead, the point has been extrapolated from the shape of the NW5 ion chamber data. The ion chamber was not absolutely calibrated before this measurement, so that the scale error between it and the NW5 scintillators is artificial. From the bare target, no reliable data was taken with the NW5 scintillators, so the ion chamber data is shown, and is also presented scaled down by the amount indicated to match the NW5 scintillator data taken during the dichromatic energy scan. Included on the figures are the Monte Carlo predictions for muon rates, described in detail in the next section.

MONTE CARLO PREDICTIONS

The Monte Carlo program HALO[9] was used to predict muon fluxes as a function of depth in the berm. Pion and kaon parents were generated according to a production model[10], followed through the magnetic elements of the dichromatic train (or were produced directly from the bare target), and were allowed to decay until they reached the hadron beam dump at NW4. Decay muons were tracked through the berm, losing energy according to an empirical dE/dx parametrization[11]. Figure 3 compares this parametrization to other recent models of energy loss[12,13,14]. It can be seen from Figure 3 that the energy loss predicted by the Monte Carlo used in these calculations is within about 7% of the highest prediction, and presents the most conservative view of energy loss in iron. HALO histograms of muon spatial distributions at the same depths in the berm as the scintillation counters then yielded the appropriate fluxes for comparison with data.

Regenerated muons (from neutrino and anti-neutrino interactions in the berm itself) are produced at a much lower rate and are not considered when comparing to data taken early in the berm. In the vicinity of the neutrino detectors, however, regenerated muons should account for a large fraction of any signal seen, since decay muons will have been ranged out by the shield. A modified form of HALO[15] has been used to predict the spectrum of muons seen in the detectors from regeneration, described in a later section.

Any decay muons which penetrate to the neutrino detectors will necessarily have been produced from parents produced at very high x_F. Very little data on particle production exists in this regime. Indeed, the particle production model used in these calculations was developed from data[16] which extended only up to $x_F = 0.7$. Comparisons of the shape of this model and high x_F data taken at 19.2 GeV at CERN[17] are shown in Figures 4 A-B. The pion data and the production model agree quite well up to x_F of 0.9. Kaon data and the production model begin to diverge above an x_F of 0.85, with the model predicting more kaons than actually observed. On an absolute scale, this production model predicts roughly a factor of two more particles produced than seen in the 19.2 GeV data, but is in agreement with other data taken at higher energies[18].

Figure 2 then shows the comparison of this Monte Carlo prediction to the shield penetration data described previously. The Monte Carlo points have been multiplied by a scale factor of 0.33, which is the average normalization of each individual comparison. Early in the berm where the shield is a well packed steel core, (NW5 and NW6) the shapes of the prediction agree fairly well with the data, although the Monte Carlo prediction is about 2.5 times higher than the measured points. Later in the berm (NW8 and the Wonder Building) where the packing fraction of the steel is not so well known and the density of the dirt is uncertain, the shapes do not agree as well, and the Monte Carlo now predicts a factor of four more muons than observed. The disparity of a factor of 2.5 early in the berm and a factor of four later in the berm between Monte Carlo and data is also seen in the bare target data.

These discrepancies can be attributed to a variety of sources.

1. There exists a large uncertainty in the over-all scale of the data.
2. The dE/dx parametrization has been checked with low energy muons only.
3. The absolute amount of matter in the middle of the berm is not well known.

In any case, it would seem that the Monte Carlo prediction errs on the conservative side, and thus should provide a safe estimate of additional shielding needed for higher energy operation.

1985 QUAD TRIPLET DATA AND REGENERATION PREDICTIONS

During the 1985 run of the quadrupole triplet train, all four experiments (E-745 in the Tohoku bubble chamber, E-744 in Lab E, E-632 in the 15-ft. bubble chamber and E-733 in Lab C) reported a large "soft" flux of particles entering their detectors. This effect was also seen by the Lab E detector in a previous wide band run at 400 GeV[19]. The nature of this soft flux was never fully understood (whether it was electro-magnetic or from slow neutrons or both) but was found to be beam associated in that it largely disappeared when the neutrino production target was taken out of the beam.

In order to reduce a buffer overflow problem in the 15-ft. EMI, the experimenters requested that some lead be placed in enclosure NW4 downstream of the hadron beam dump. Subsequently, a plug of lead comprising 158 metric tons was installed and arranged in a rough cylinder of diameter 1.8 m and depth 5.5 m. The 15-ft. experimenters reported a 20% improvement in the EMI rate after the lead installation. Other experimenters did not provide quantitative numbers, but indicated some improvement.

No on-line muon rate measurements were reported by any experiments. Following the run, data was furnished by the 15-ft. experimenters[20] on muon fluxes in the chamber under a variety of operating conditions. Besides the installation of the lead plug, two other factors contributed substantially to the muon rates observed. These were the polarity of the Lab E toroid upstream of the chamber, and whether the NWest test line was on or off. These effects can be seen in Figures 5 and 6. These and subsequent figures have 4 separate momentum ranges plotted for both positive and negative muons; below 20 GeV, 20-100 GeV, 100-200 GeV and greater than 200 GeV.

Figure 5 illustrates that the total muon rates can change by a factor of 3 and the composition between + or - can change drastically depending on the Lab E toroid polarity. Figure 6 illustrates that the muon rates seen in the chamber for momenta below 20 GeV can change by a factor of 2 depending on the status of the NWest test beam[21]. No data is available on NWest status after the lead plug was installed, however, the very low rate observed below 20 GeV favors NW mostly off for these data. This will be assumed in order to normalize the regeneration Monte Carlo.

Figures 7 shows Monte Carlo calculations of expected muon distributions (+/-) in the 15-ft. chamber for the Lab E toroid focussing mu+ and mu-. Added together in the distributions are the muons calculated from regeneration in the berm and those expected from decay punch-through of the berm with the additional 5.5 m lead plug (a small contribution). The muons from the regeneration Monte Carlo have been normalized to the 5.5 m data from 20 to 100 GeV, and needed to be multiplied by a factor of 2. The decay muons were multiplied by a factor of 0.33, the average normalization of the Monte Carlo to the data found for Figure 2. Figure 7, then, is directly comparable to the data shown in Figure 5.

Tables I and II show the spatial distribution of muons and their average energy over an area 9 times bigger than the chamber, and centered on the chamber, for muons produced by punch-through and by regeneration, respectively. During the run, the 15-ft. field was set to sweep positive particles west. Since neither punch-through nor regenerated muons are distributed uniformly in space, some shifting in the population of the lowest momentum bins might occur.

Figure 8 illustrates the depletion of muon rates by the addition of the 5.5 m lead plug. These Monte Carlo calculations (both regeneration and decay punch-through) have been normalized using the same prescription as for Figure 7. Figure 8 is directly comparable to the NWest test beam "off" condition shown in the data of Figure 6.

It can be seen by inspection of Figures 5-8 that the Monte Carlo calculations model the data to within a factor of 2 or so, and should thus provide a reasonable model for extrapolation to higher energy operation.

SHIELDING NEEDED FOR HIGHER ENERGY OPERATION

The Monte Carlo has been run for the quadrupole triplet train, changing the energy of the primary beam on target, and for a set of different lengths of lead installed in enclosure NW4. This is shown graphically in Figure 9, for positive kaon parents. (Positive pion parents contribute an equal flux of muons, and thus the scale shown can be considered a reasonable prediction of the absolute number of muons produced by decay punch-through. Negative parents contribute only about 10% more punch-through.) It can be seen that a length of lead of 16-18 m should produce about the same number of punch-through muons for 900+ GeV primary protons as were seen at 800 GeV. (Additional calculations show that regenerated muons should be about 33% higher at 900 GeV and about 50% higher at 1000 GeV than at 800 GeV.)

It should be pointed out that the amount and composition of materials in the berm is known only approximately. The Monte Carlo calculations shown have assumed that the 1980 steel addition to the berm was installed with a 90% packing fraction, and that the density of dirt in the berm is 2.25 gm/cm^3. Inspection of the installation drawings indicates that the packing fraction could be close to 100%. When a decay Monte Carlo with a packing fraction of 97% was run, the best agreement to the data was obtained with a dirt density of 2.0 gm/cm^3. These calculations are compared to the muon penetration data in Figure 10, where here the Monte Carlo points have been scaled by an average factor of 0.25. Although the 90% packing fraction model gives a better agreement with the data at low dichromatic train energies (Figure 2), the 97% model can not be ruled out. Figure 11 shows the decay punch-through predictions for the 97% berm model, as a function of primary beam energy and lead shield length. The absolute rate of muons at the end of the berm is about 3 times greater than the 90% model (and thus about 9 times greater than the observed 15-ft. bubble chamber data). The relative behavior, however, as a function of energy and lead length is the same. Since the scale of data to Monte Carlo for the 90% model is roughly constant regardless of depth in the berm, and since a density of 2.25 gm/cm^3 more closely matches core samples[22], it has been chosen as a best description of the Fermilab neutrino berm.

Enough steel encased lead has been located to extend the existing plug by 2.9m. At the beginning of 1986, Fermilab inventory contained 140 metric tons of lead in the form of 29.5 kg ingots or "pigs". These have been hand-stacked upstream of the steel encased plug to extend the shield an amount equivalent to 4.3 m of lead, bringing the total lead addition to 12.7m. Another 182 metric tons of lead has been purchased from the DOE lead bank and installed bringing the 1.8 m diameter lead shield addition to a total length of about 18.3m.

REFERENCES

1. S. Mori, "Muon Shield for the Tevatron at Fermilab", Fermilab technical memo TM-790, May 1978; and S. Mori, "Muon Shield for the Tevatron (II)", Fermilab technical memo TM-843, January, 1979.

2. L. Stutte, "Further Design Studies for a Tevatron Era Dichromatic Beam", Fermilab technical memo TM-1091, January, 1982; and L. Stutte, "The NCI Dichromatic Beam Tests", Fermilab technical memo TM-1391, March, 1986.

3. Participants in these measurements were D. Owen, Michigan State University, and S. Pordes, P. Rapidis and L. Stutte, Fermilab.

4. L. Stutte, "NCenter Wide Band Neutrino Beam", Fermilab technical memo TM-1306, March, 1985.

5. P. Auchincloss, et. al., "Design, Construction, and Calibration of Large Ion Chambers for Muon Flux Monitoring in Neutrino Beams at Fermilab", Fermilab note FN-382, March, 1983.

6. The counters were on loan for these tests from Fermilab experiment E-665.

7. I. E. Stockdale, et. al., "Limits on Muon-Neutrino Oscillations in the Mass Range 30 - 1000 eV^2/c^4", Physical Review Letters 52 ,1384, 1984.

8. Secondary Emission Monitor, made by L. N. D. Inc., 3230 Lawson Blvd., Ocean Side, New York, 11572.

9. Ch. Iselin, "HALO, A Computer Program to Calculate Muon Halo", CERN Report 74-17, 1974.

10. A. J. Malensek, "Empirical Formula for Thick Target Production", Fermilab note FN-341, 1981.

11. Marshall Mugge, private communication.

12. W. Lohman, R. Kopp and R. Voss, "Energy Loss Tables for Muons in the Energy Range 1-10000 GeV", CERN Report 85-03. This model has been favorably compared to data taken by the BCDMS Muon Collaboration in R. Kopp, et. al., "A Measurement of Energy Loss Distributions of Energetic Muons in Iron", Zeitschrift fur Physik C 28 ,171,1985.

13. G. Koizumi, "Muon dE/dx and Range Tables for Tevatron Energies: Results for Some Shielding Materials", Fermilab technical memo TM-786, May, 1979.

14. C. Baltay, et. al., "The Design of the Magnetized Muon Shield for the Prompt Neutrino Facility", Fermilab technical memo TM-1155, October, 1982.

15. Dave Carey, private communication.

16. This model (reference 10) was normalized to data taken from H. W. Atherton, et. al., CERN Report 80-07, 1980.

17. Data taken from CERN Report 70-12, 1970.

18. M. Bourquin, et. al., "Particle and Antiparticle Production by 200 GeV/c Protons in the Charged Hyperon Beam at the CERN SPS",Nuclear Physics B 153 ,13,1979.

19. Arie Bodek, private communication.

20. Data supplied by Michael Jones, E-632 collaboration.

21. NWest conditions furnished by John Cooper, CDF collaboration.

22. Thornton Murphy, private communication.

TABLE I.

Spatial Distribution of Muons Produced
by Decay Punch-through of the Berm
at 800 GeV - 0.0 m of lead

Positive and Negative Muons Summed - Lab E Toroid Off

NUMBER OF MUONS PER 10^{12} PROTONS IN 3 m x 3 m AREAS
CENTERED ON THE 15-FT. BUBBLE CHAMBER
(and their average momentum in GeV)

	EAST	CENTER	WEST
TOP	20.08 +/- 2.24 (15.19 GeV)	26.31 +/- 2.58 (17.89 GeV)	28.25 +/- 2.69 (15.06 GeV)
CENTER	13.99 +/- 1.88 (17.13 GeV)	6.02 +/- 1.24 (12.63 GeV)	16.32 +/- 2.04 (16.90 GeV)
BOTTOM	0.58 +/- 0.38 (5.51 GeV)	0.31 +/- 0.26 (11.86 GeV)	0.90 +/- 0.47 (5.58 GeV)

TABLE II.

Spatial Distribution of Muons Produced
by Regeneration in the Berm
at 800 GeV - 0.0 m of lead

Positive and Negative Muons Summed - Lab E Toroid Off

NUMBER OF MUONS PER 10^{12} PROTONS IN 3 m x 3 m AREAS
CENTERED ON THE 15-FT. BUBBLE CHAMBER
(and their average momentum in GeV)

	EAST	CENTER	WEST
TOP	0.56 +/- 0.06 (51.9 GeV)	0.70 +/- 0.06 (73.2 GeV)	0.44 +/- 0.06 (55.0 GeV)
CENTER	0.86 +/- 0.08 (62.8 GeV)	3.50 +/- 0.16 (88.3 GeV)	0.76 +/- 0.08 (74.1 GeV)
BOTTOM	0.38 +/- 0.06 (43.0 GeV)	0.81 +/- 0.08 (53.7 GeV)	0.32 +/- 0.04 (40.8 GeV)

FIGURE CAPTIONS

1. Layout of the Neutrino Area at Fermilab showing the location of monitors used in this measurement.

2. Muon rates observed at different dichromatic train settings and for the bare target (plotted at 0 GeV), as a function of depth in the berm, compared to Monte Carlo predictions.

3. The dE/dx parametrization used in these calculations compared to other recent models.

4. Production data at high x_F compared to the model used in these calculations. A) Pions and B) Kaons.

5. Muon rates observed in the 15-ft. bubble chamber in various momentum ranges, as a function of the polarity of the Lab E toroid, after the insertion of the 5.5 m lead plug.

6. Muon rates observed in the 15-ft. bubble chamber in various momentum ranges, as a function of the NWest test beam status before the insertion of a lead plug in NW4, and for an unknown NWest condition after the 5.5 m lead plug was installed. The Lab E toroid was set to focus positive muons for all this data.

7. Monte Carlo predictions of muon rates in the 15-ft. bubble chamber in various momentum ranges, as a function of the polarity of the Lab E toroid, after the installation of the 5.5 m lead plug. Both regenerated and decay punch-through muons are included.

8. Monte Carlo predictions of muon rates in the 15-ft. bubble chanber in various momentum ranges, before and after the insertion of the 5.5 m lead plug. The Lab E toroid was set to focus positive muons. Both regenerated and decay punch-through muons are included.

9. Monte Carlo predictions of muon punch-through rates for the 15-ft. bubble chamber as a function of primary proton energy and for various lengths of lead in NW4.

10. Muon rates observed at different dichromatic train settings and for the bare target (plotted at 0 GeV), as a function of depth in the berm, compared to Monte Carlo predictions for a berm with 97% steel packing fraction and a dirt density of 2.0 gm/cm^3.

11. Monte Carlo predictions of muon punch-through rates for the 15-ft. bubble chamber as a function of primary proton energy and for various lengths of lead in NW4, for a berm with 97% steel packing fraction and a dirt density of 2.0 gm/cm^3.

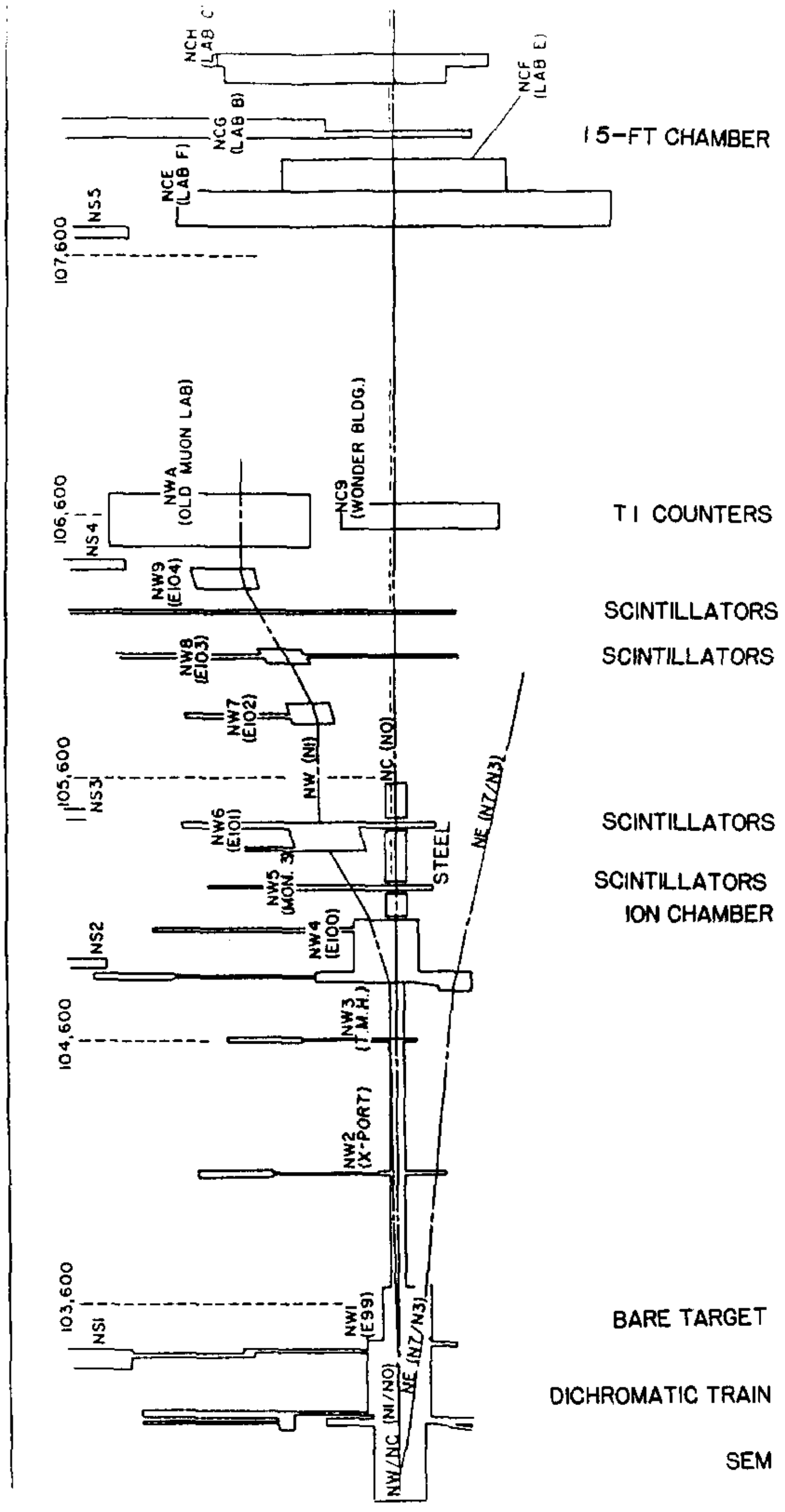
15-FT CHAMBER
T1 COUNTERS
SCINTILLATORS
SCINTILLATORS
SCINTILLATORS
SCINTILLATORS
ION CHAMBER
BARE TARGET
DICHROMATIC TRAIN
SEM
NCH (LAB C)
NCF (LAB E)
NCG (LAB B)
NCE (LAB F)
NS5
107,600
NWA (OLD MUON LAB)
NC9 (WONDER BLDG.)
106,600
NS4
NW9 (E104)
NW8 (E103)
NW7 (E102)
NC (NO)
NW (N1)
105,600
NS3
NW6 (E101)
STEEL
NE (N2/N3)
NW5 (MON. 3)
NW4 (E100)
NS2
104,600
NW3 (T.M.H.)
NW2 (X-PORT)
103,600
NS1
NW1 (E99)
NE (N2/N3)
NW/NC (N1/NO)

FIGURE I

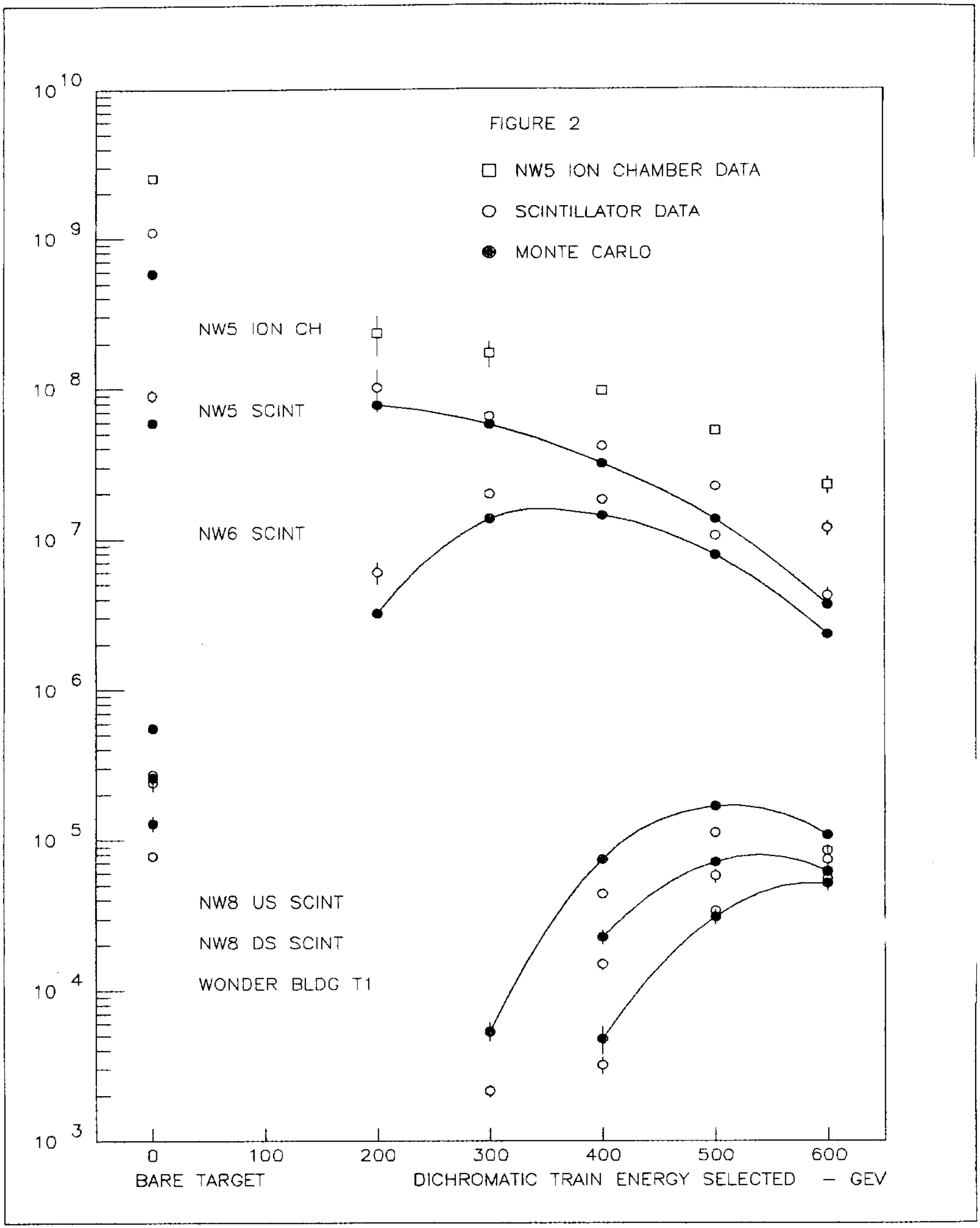
FIGURE 2
NW5 ION CHAMBER DATA
SCINTILLATOR DATA
MONTE CARLO
NW5 ION CH
NW5 SCINT
NW6 SCINT
NW8 US SCINT
NW8 DS SCINT
WONDER BLDG T1
10^{10}
10^{9}
10^{8}
10^{7}
10^{6}
10^{5}
10^{4}
10^{3}
0
100
200
300
400
500
600
BARE TARGET
DICHROMATIC TRAIN ENERGY SELECTED – GEV

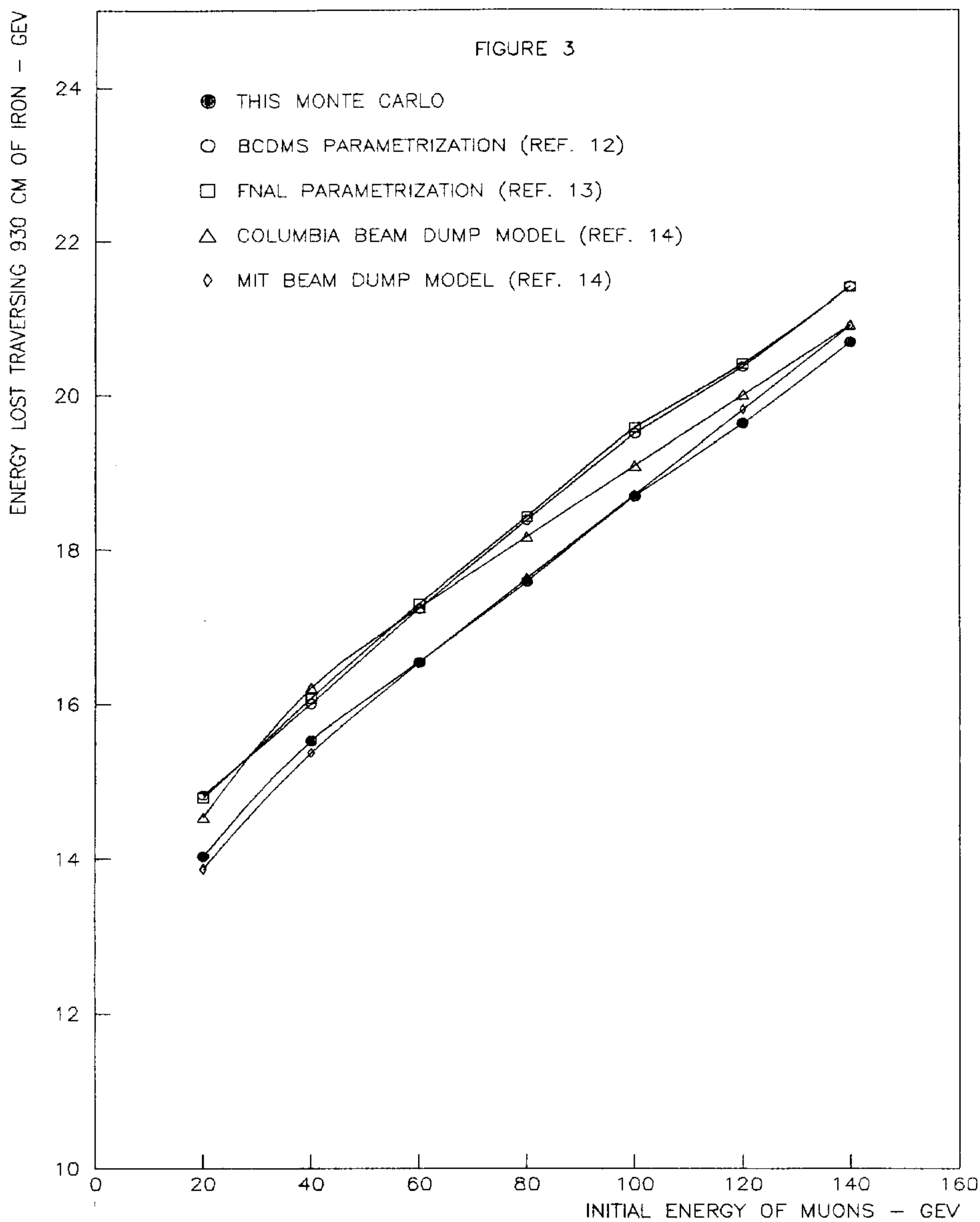
FIGURE 3
THIS MONTE CARLO
BCDMS PARAMETRIZATION (REF. 12)
FNAL PARAMETRIZATION (REF. 13)
COLUMBIA BEAM DUMP MODEL (REF. 14)
MIT BEAM DUMP MODEL (REF. 14)
ENERGY LOST TRAVERSING 930 CM OF IRON - GEV
INITIAL ENERGY OF MUONS - GEV
10
12
14
16
18
20
22
24
0
20
40
60
80
100
120
140
160

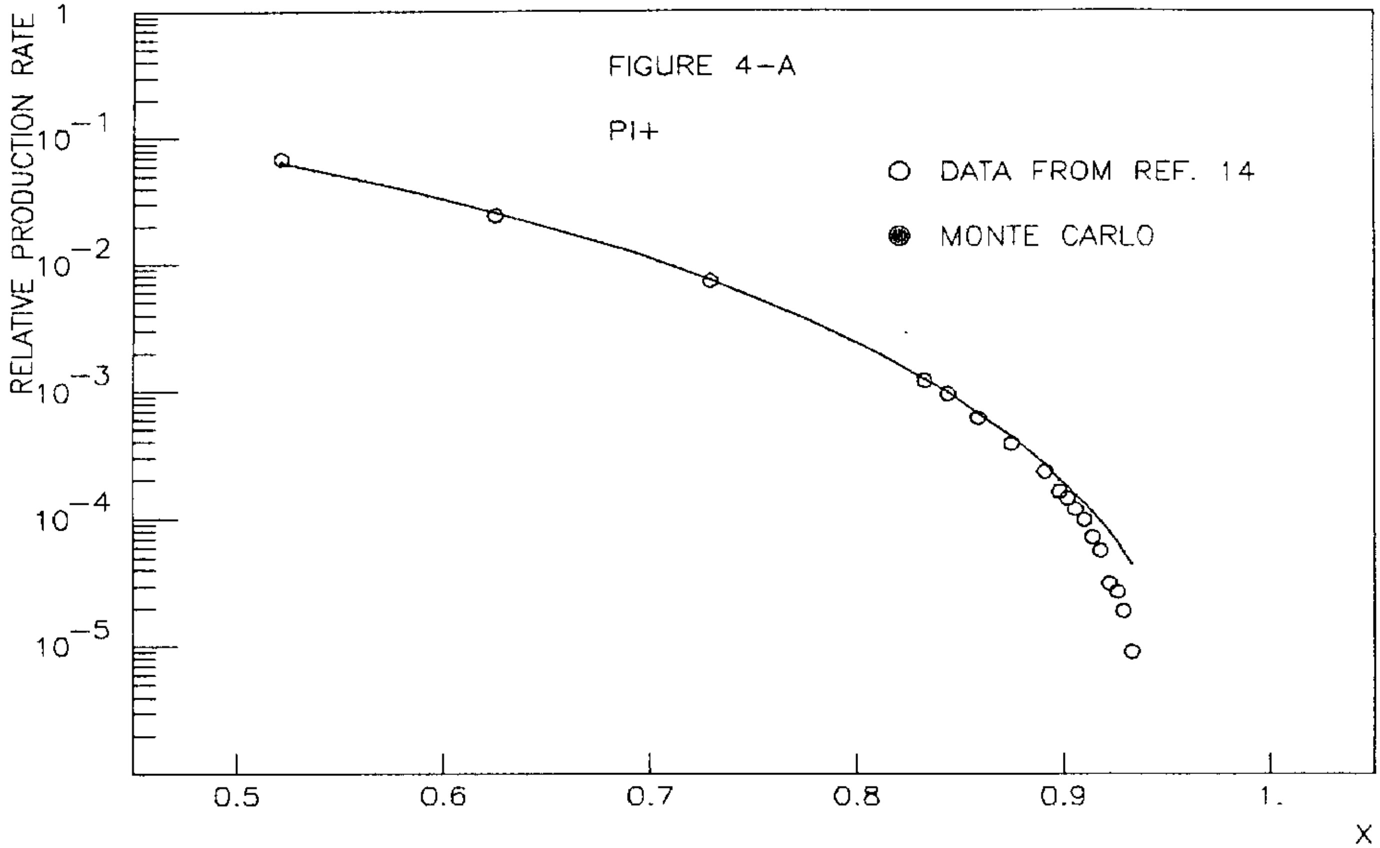
FIGURE 4-A
PI+
DATA FROM REF. 14
MONTE CARLO
RELATIVE PRODUCTION RATE
1
10^{-1}
10^{-2}
10^{-3}
10^{-4}
10^{-5}
0.5
0.6
0.7
0.8
0.9
1.
X

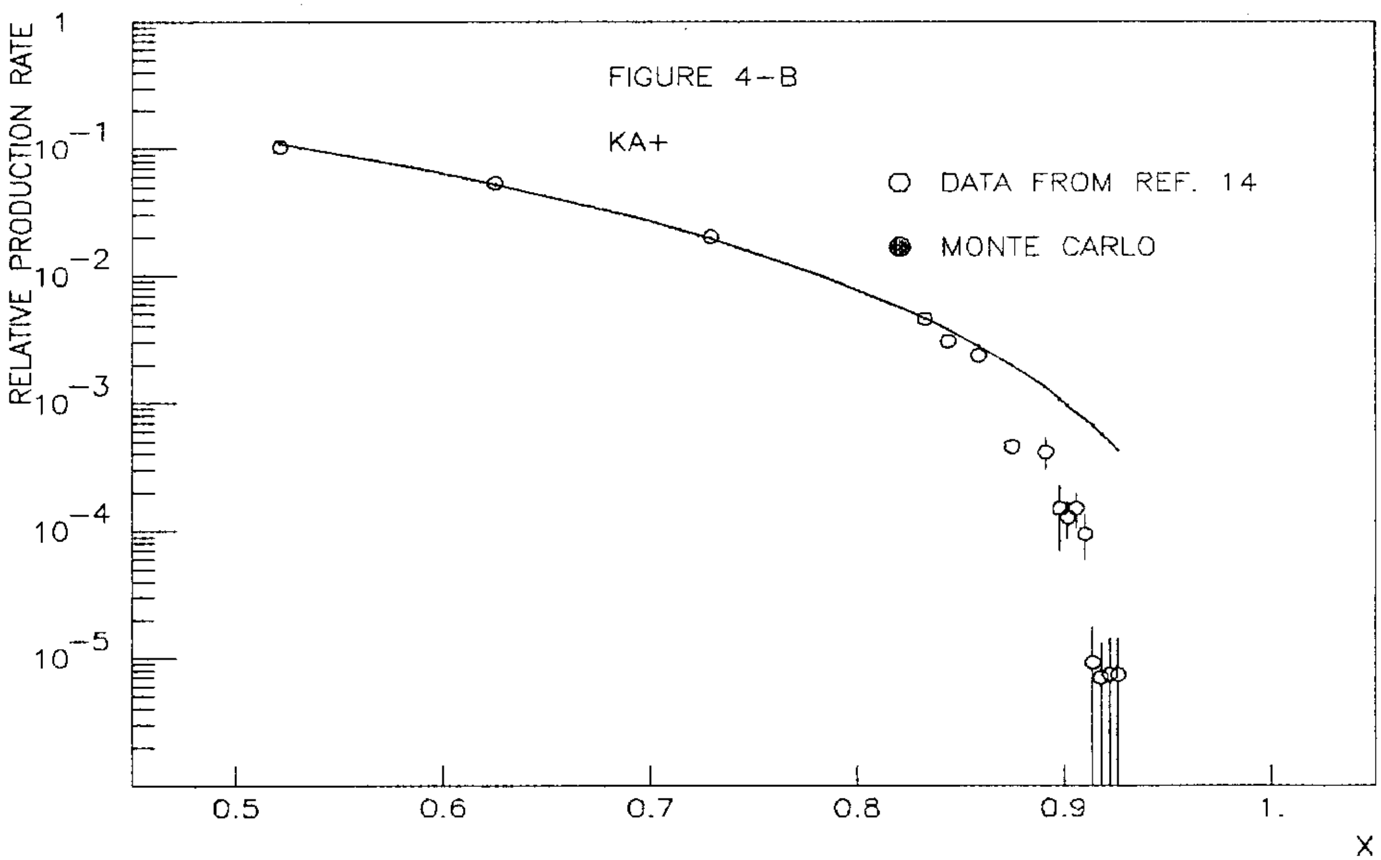
FIGURE 4-B
KA+
DATA FROM REF. 14
MONTE CARLO
RELATIVE PRODUCTION RATE
1
10^{-1}
10^{-2}
10^{-3}
10^{-4}
10^{-5}
0.5
0.6
0.7
0.8
0.9
1.
X

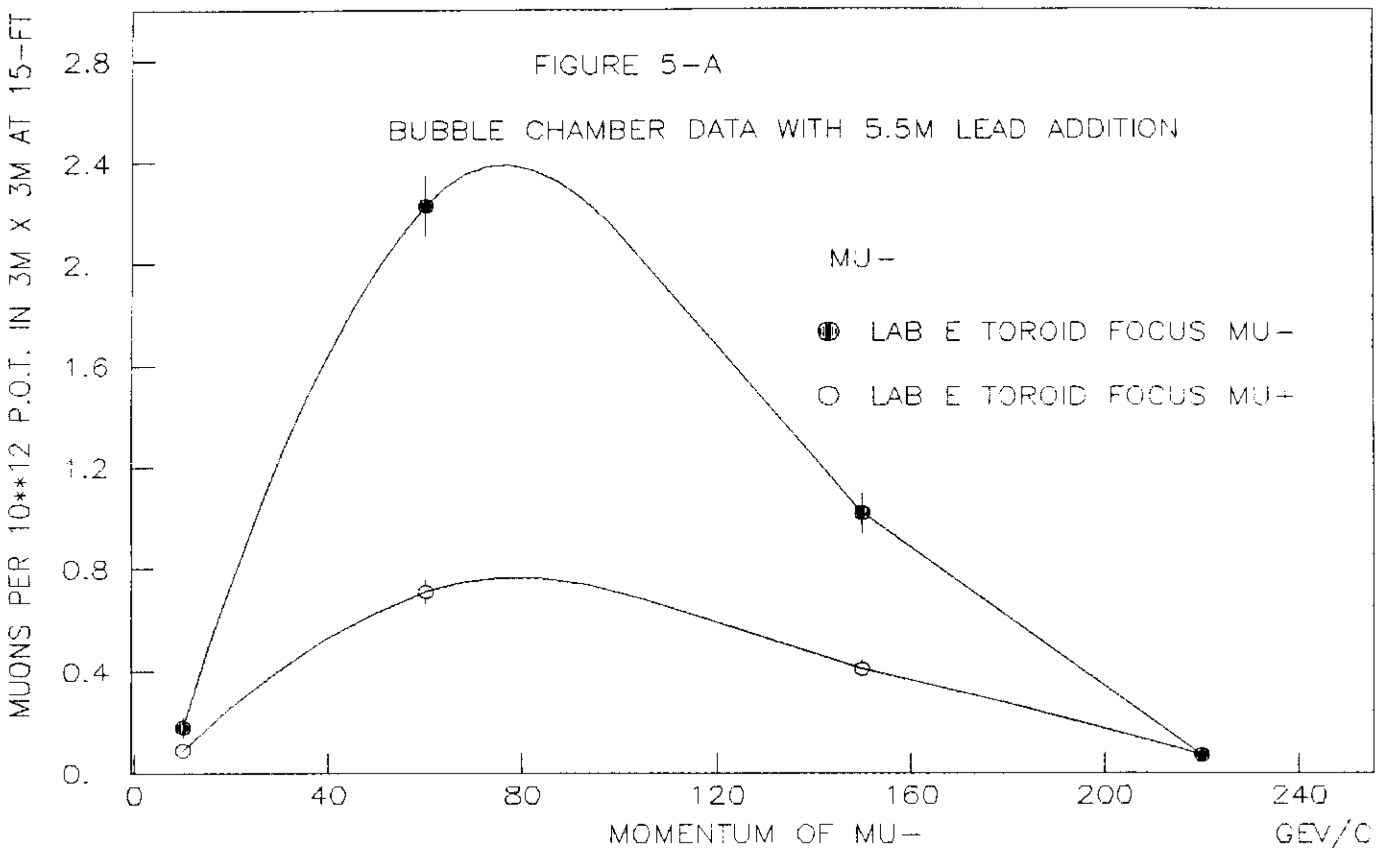
FIGURE 5-A
BUBBLE CHAMBER DATA WITH 5.5M LEAD ADDITION
MU-
LAB E TOROID FOCUS MU-
LAB E TOROID FOCUS MU+
MUONS PER 10**12 P.O.T. IN 3M X 3M AT 15-FT
0. 0.4 0.8 1.2 1.6 2. 2.4 2.8
0 40 80 120 160 200 240
MOMENTUM OF MU-
GEV/C

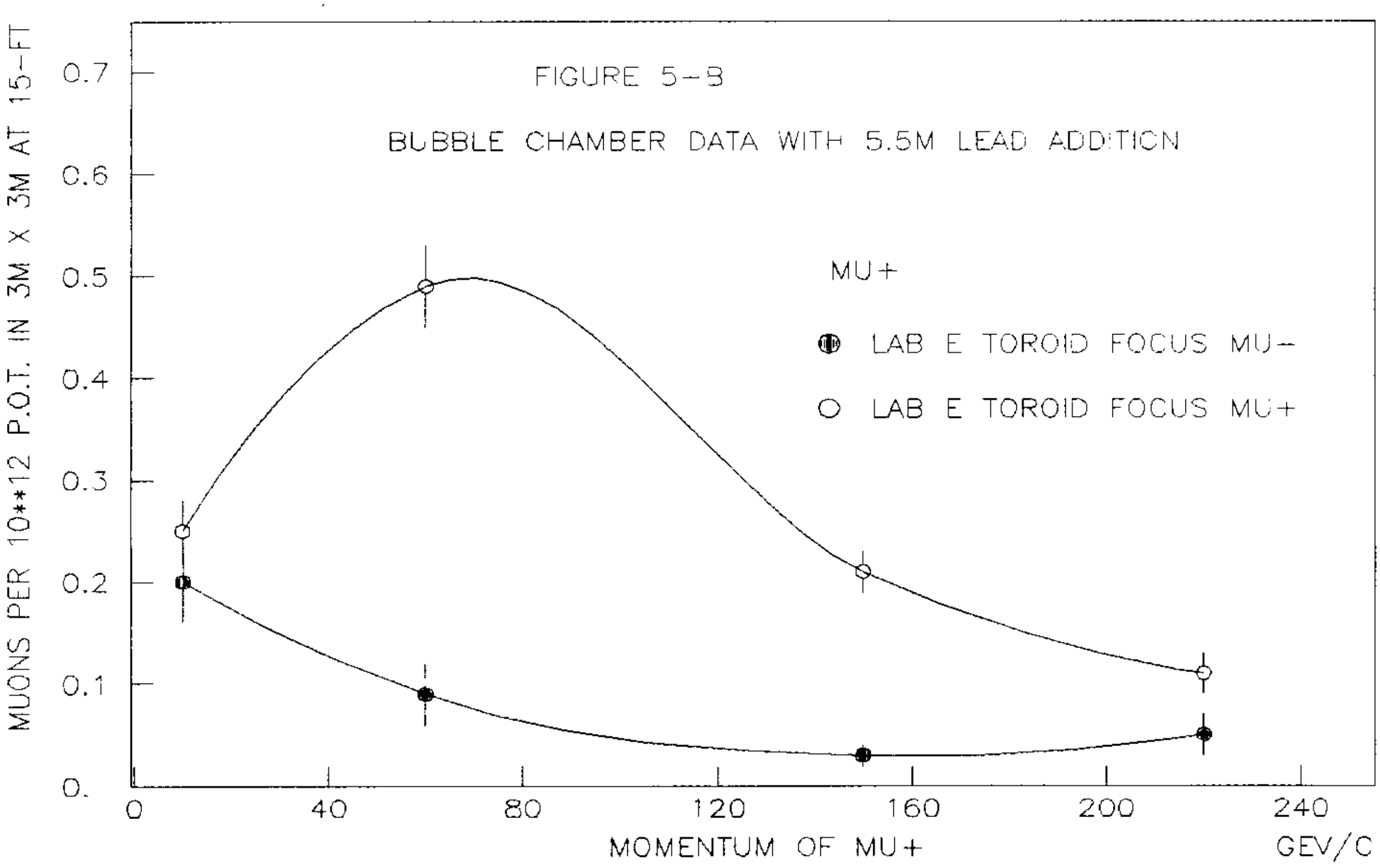
FIGURE 5-B
BUBBLE CHAMBER DATA WITH 5.5M LEAD ADDITION
MU+
LAB E TOROID FOCUS MU-
LAB E TOROID FOCUS MU+
MUONS PER 10**12 P.O.T. IN 3M X 3M AT 15-FT
0. 0.1 0.2 0.3 0.4 0.5 0.6 0.7
0 40 80 120 160 200 240
MOMENTUM OF MU+
GEV/C

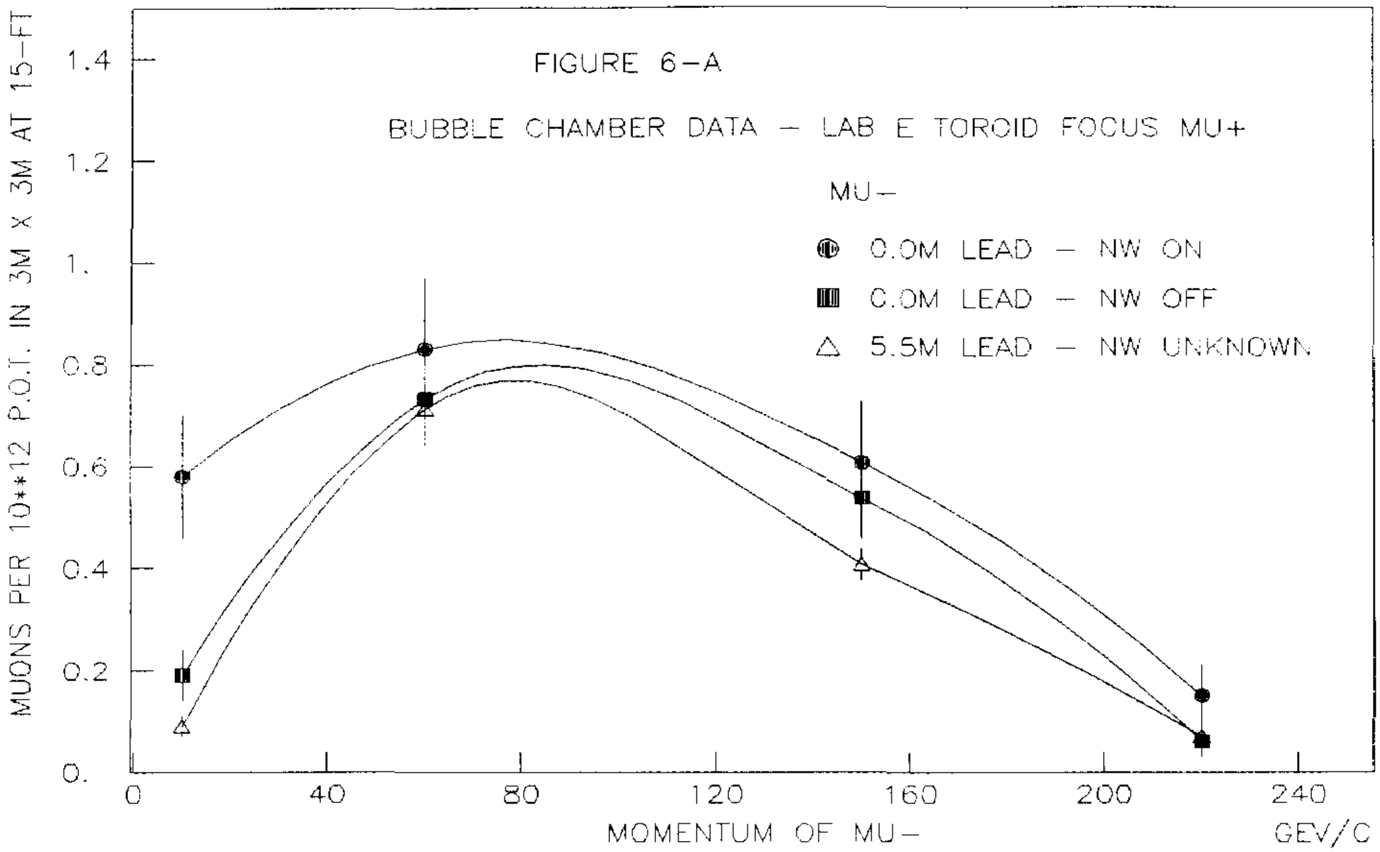
FIGURE 6-A
BUBBLE CHAMBER DATA – LAB E TOROID FOCUS MU+
MU–
0.0M LEAD – NW ON
0.0M LEAD – NW OFF
5.5M LEAD – NW UNKNOWN
MUONS PER 10**12 P.O.T. IN 3M X 3M AT 15-FT
MOMENTUM OF MU–
GEV/C
0.
0.2
0.4
0.6
0.8
1.
1.2
1.4
0
40
80
120
160
200
240

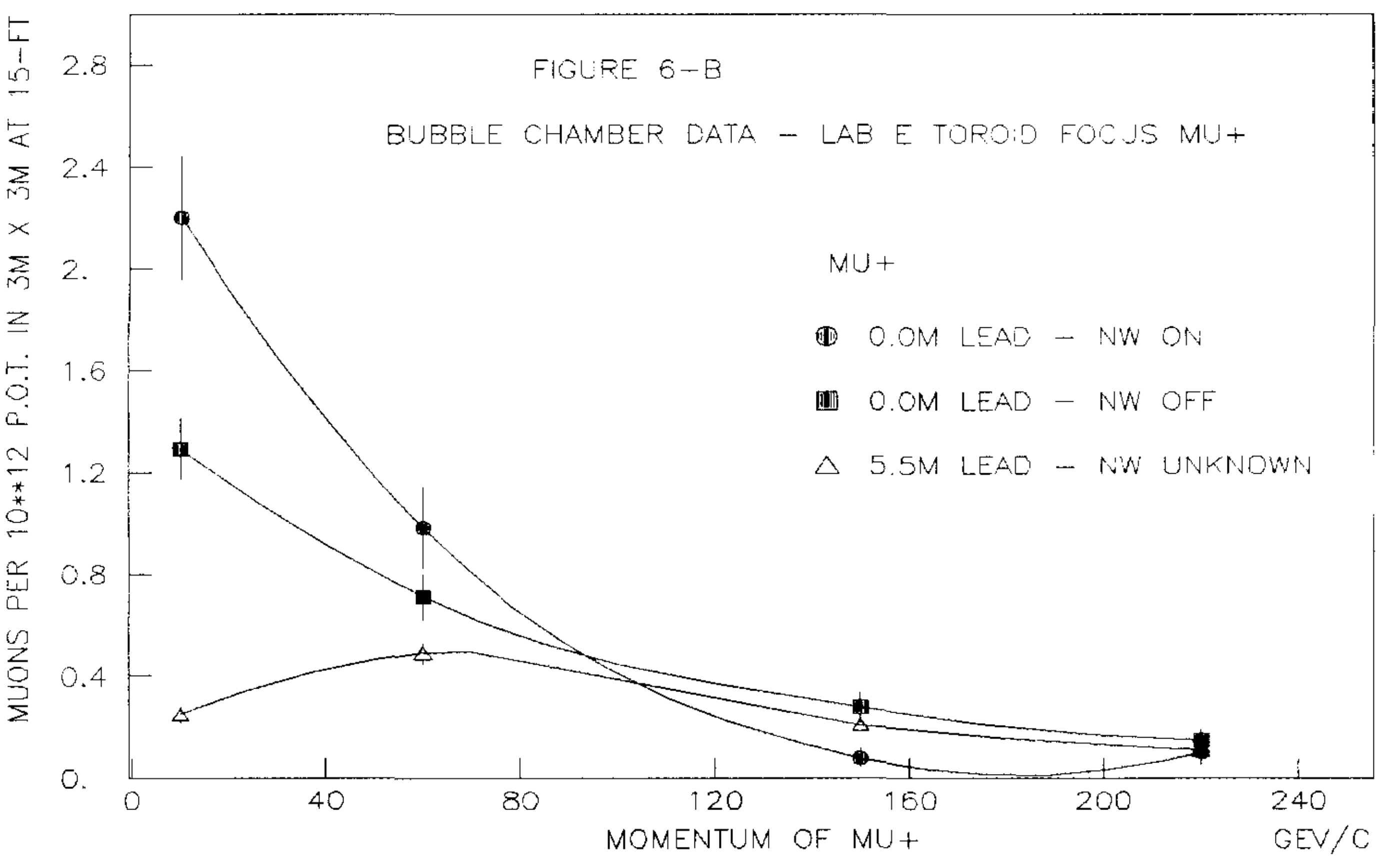
FIGURE 6-B
BUBBLE CHAMBER DATA – LAB E TOROID FOCUS MU+
MU+
0.0M LEAD – NW ON
0.0M LEAD – NW OFF
5.5M LEAD – NW UNKNOWN
MUONS PER 10**12 P.O.T. IN 3M X 3M AT 15-FT
MOMENTUM OF MU+
GEV/C
0.
0.4
0.8
1.2
1.6
2.
2.4
2.8
0
40
80
120
160
200
240

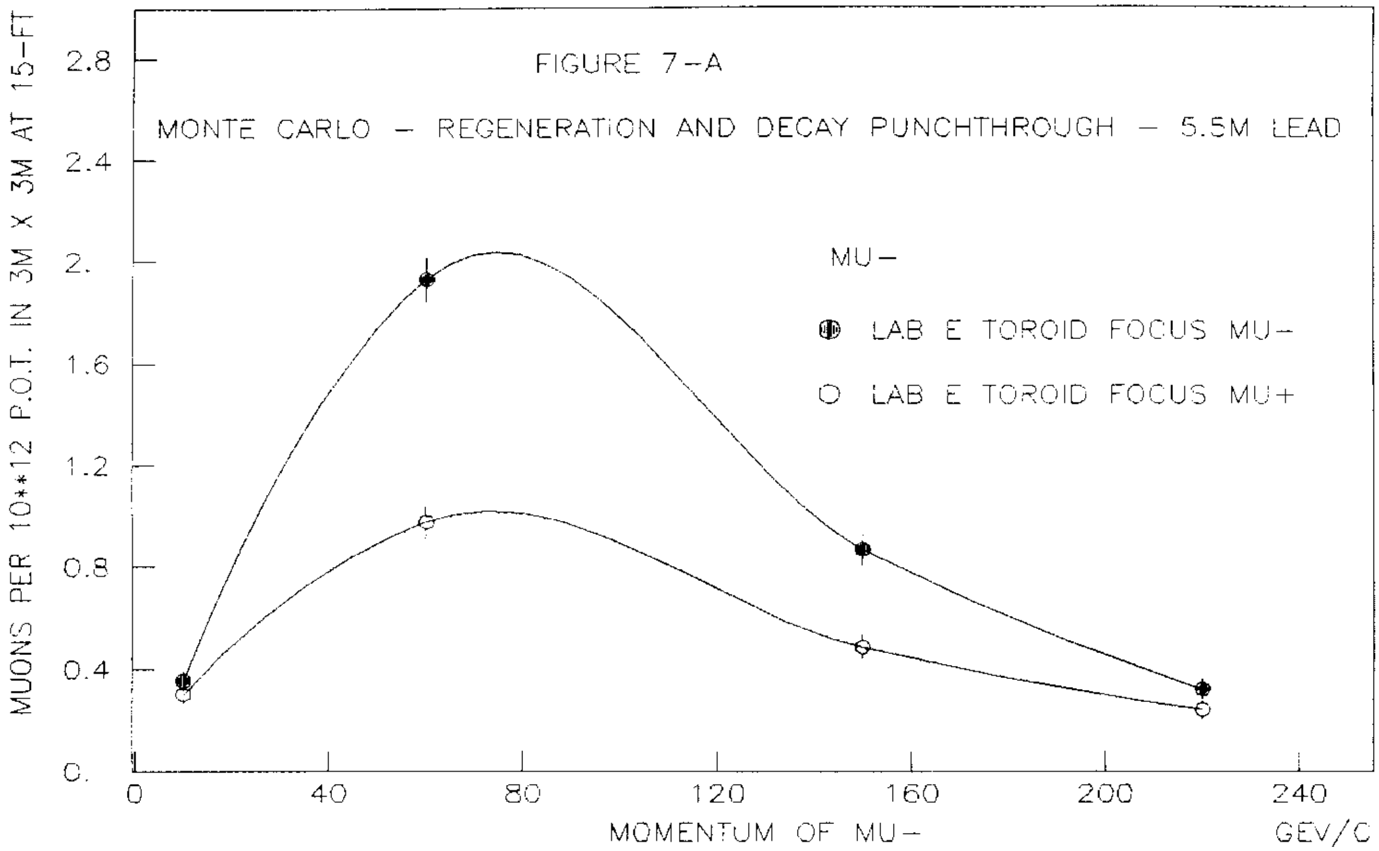
FIGURE 7-A
MONTE CARLO - REGENERATION AND DECAY PUNCHTHROUGH - 5.5M LEAD
MU-
LAB E TOROID FOCUS MU-
LAB E TOROID FOCUS MU+
MUONS PER 10**12 P.O.T. IN 3M X 3M AT 15-FT
0.
0.4
0.8
1.2
1.6
2.
2.4
2.8
0
40
80
120
160
200
240
MOMENTUM OF MU-
GEV/C

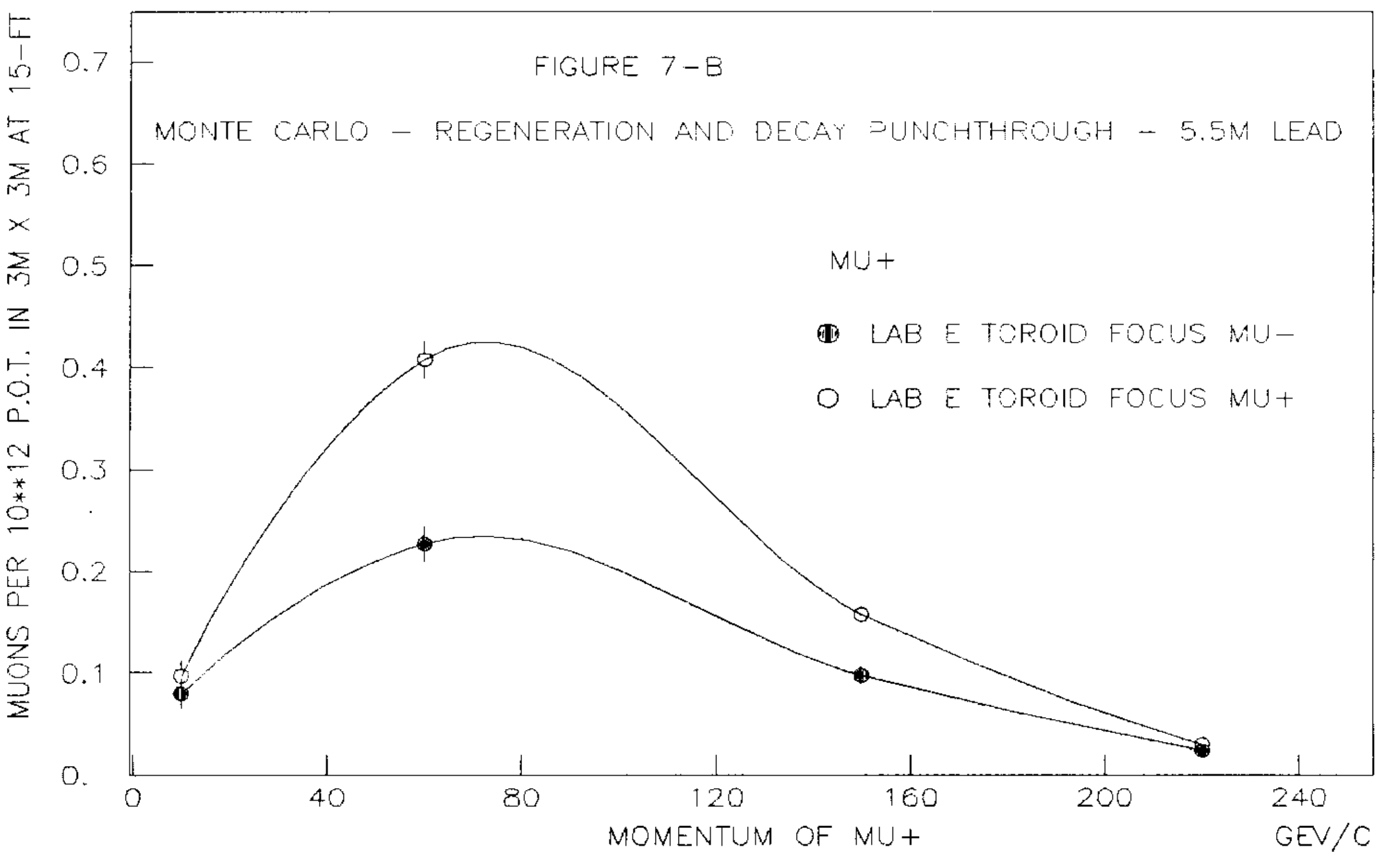
FIGURE 7-B
MONTE CARLO - REGENERATION AND DECAY PUNCHTHROUGH - 5.5M LEAD
MU+
LAB E TOROID FOCUS MU-
LAB E TOROID FOCUS MU+
MUONS PER 10**12 P.O.T. IN 3M X 3M AT 15-FT
0.
0.1
0.2
0.3
0.4
0.5
0.6
0.7
0
40
80
120
160
200
240
MOMENTUM OF MU+
GEV/C

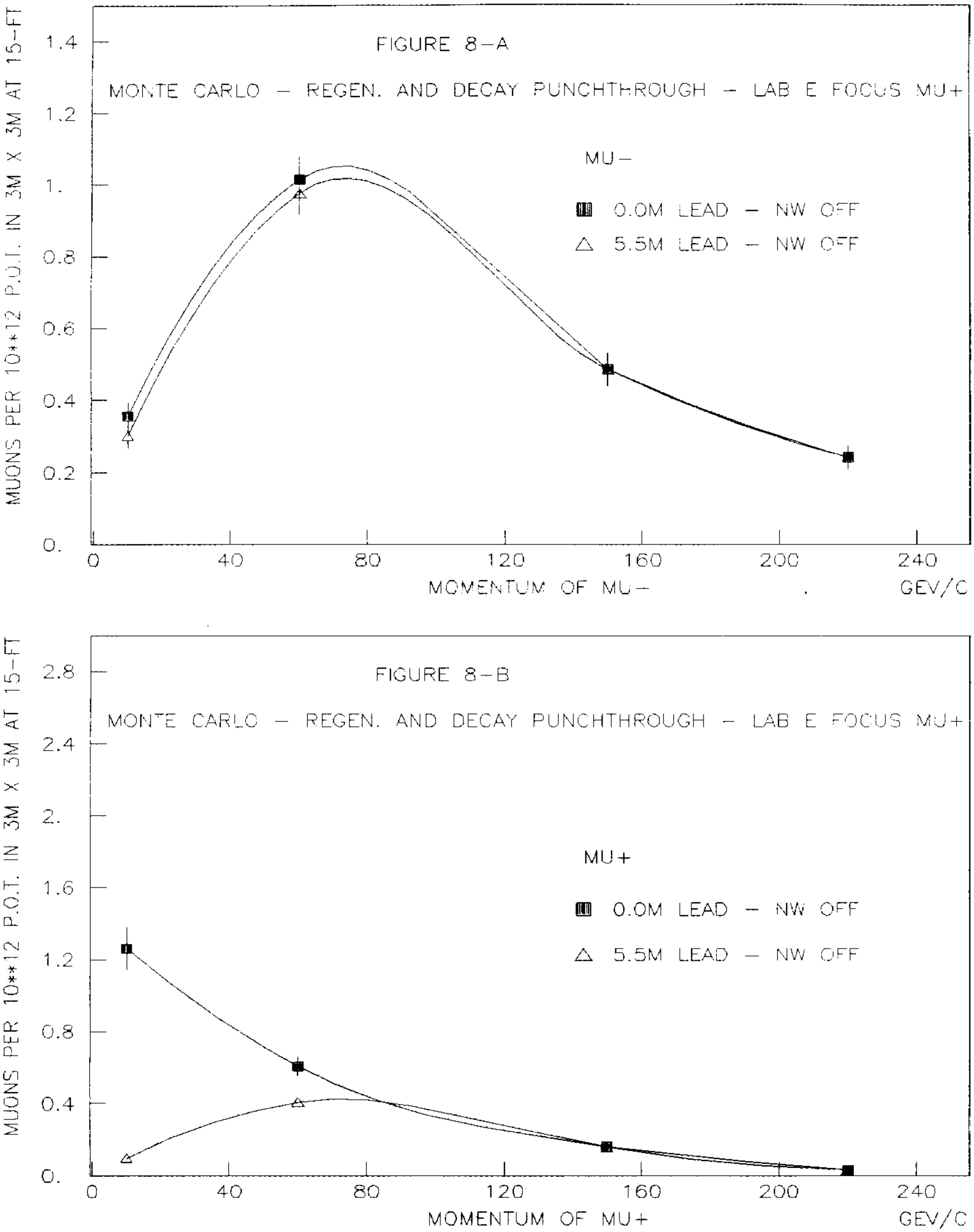
FIGURE 8-A
MONTE CARLO - REGEN. AND DECAY PUNCHTHROUGH - LAB E FOCUS MU+
MU-
0.0M LEAD - NW OFF
5.5M LEAD - NW OFF
MUONS PER 10**12 P.O.T. IN 3M X 3M AT 15-FT
1.4
1.2
1.
0.8
0.6
0.4
0.2
0.
0
40
80
120
160
200
240
MOMENTUM OF MU-
GEV/C
FIGURE 8-B
MONTE CARLO - REGEN. AND DECAY PUNCHTHROUGH - LAB E FOCUS MU+
MU+
0.0M LEAD - NW OFF
5.5M LEAD - NW OFF
MUONS PER 10**12 P.O.T. IN 3M X 3M AT 15-FT
2.8
2.4
2.
1.6
1.2
0.8
0.4
0.
MOMENTUM OF MU+
GEV/C

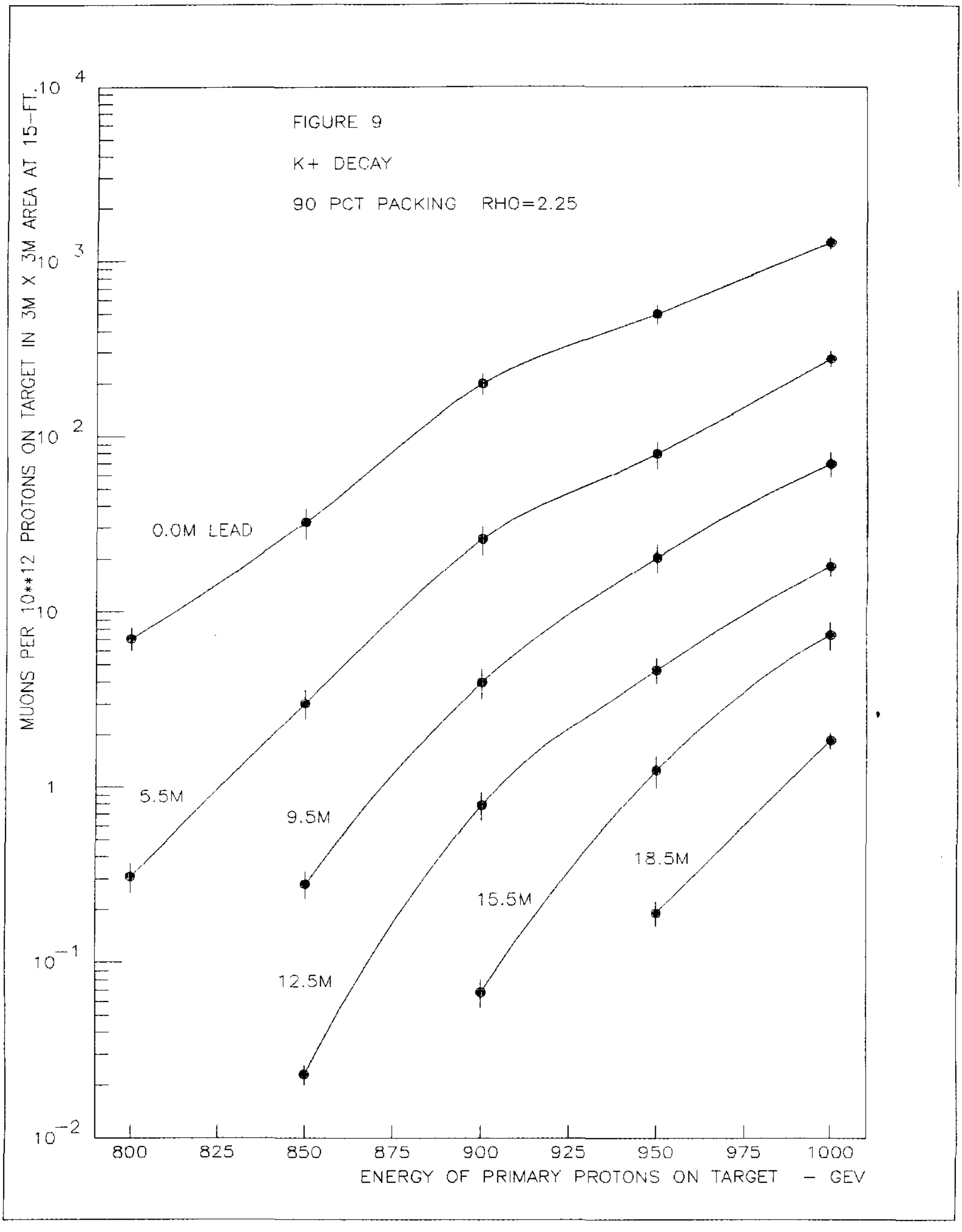
FIGURE 9
K+ DECAY
90 PCT PACKING RHO=2.25
0.0M LEAD
5.5M
9.5M
12.5M
15.5M
18.5M
MUONS PER 10**12 PROTONS ON TARGET IN 3M X 3M AREA AT 15-FT.
ENERGY OF PRIMARY PROTONS ON TARGET - GEV
800
825
850
875
900
925
950
975
1000
10^{-2}
10^{-1}
1
10
10^{2}
10^{3}
10^{4}

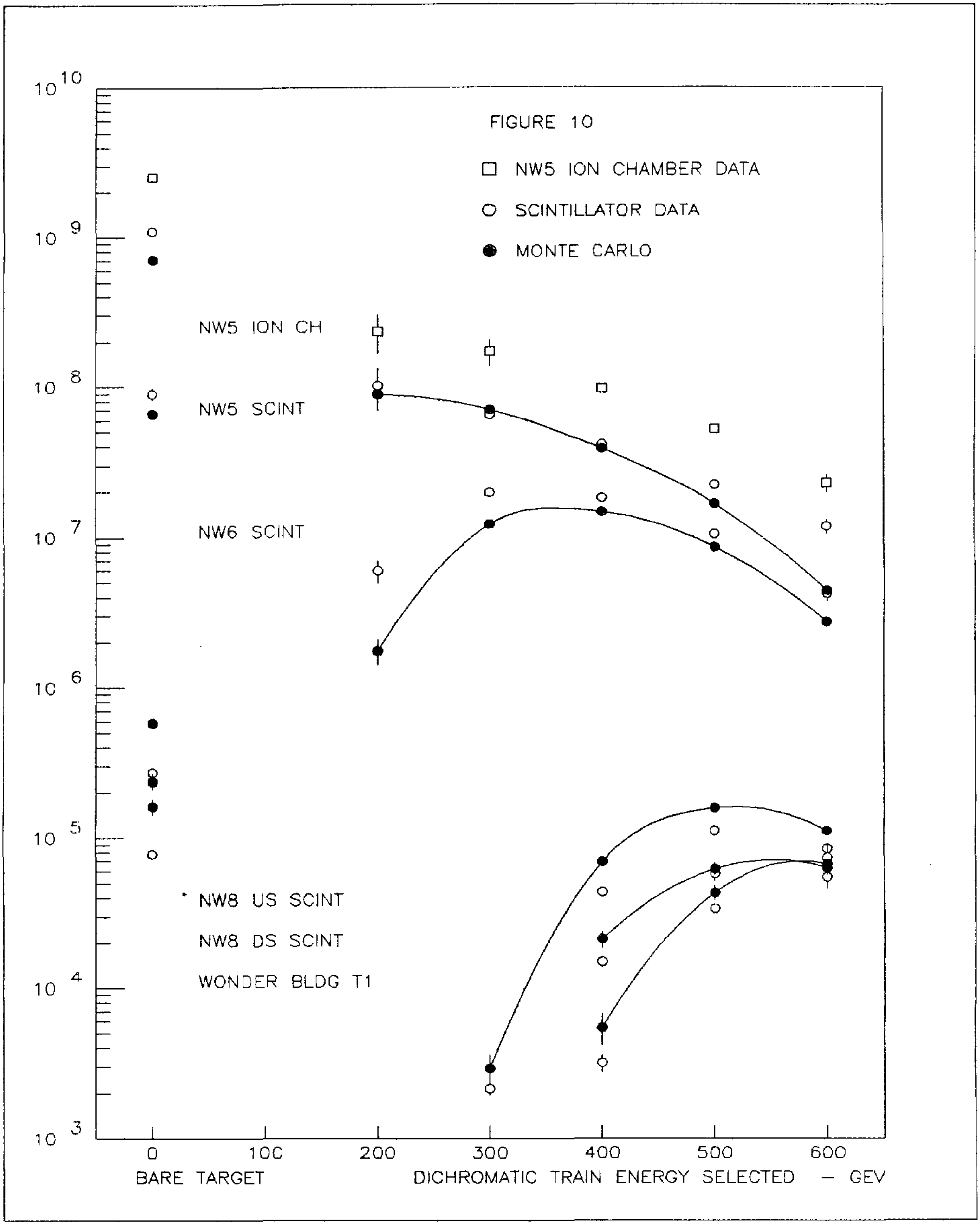
FIGURE 10
NW5 ION CHAMBER DATA
SCINTILLATOR DATA
MONTE CARLO
NW5 ION CH
NW5 SCINT
NW6 SCINT
NW8 US SCINT
NW8 DS SCINT
WONDER BLDG T1
10 10
10 9
10 8
10 7
10 6
10 5
10 4
10 3
0
100
200
300
400
500
600
BARE TARGET
DICHROMATIC TRAIN ENERGY SELECTED — GEV

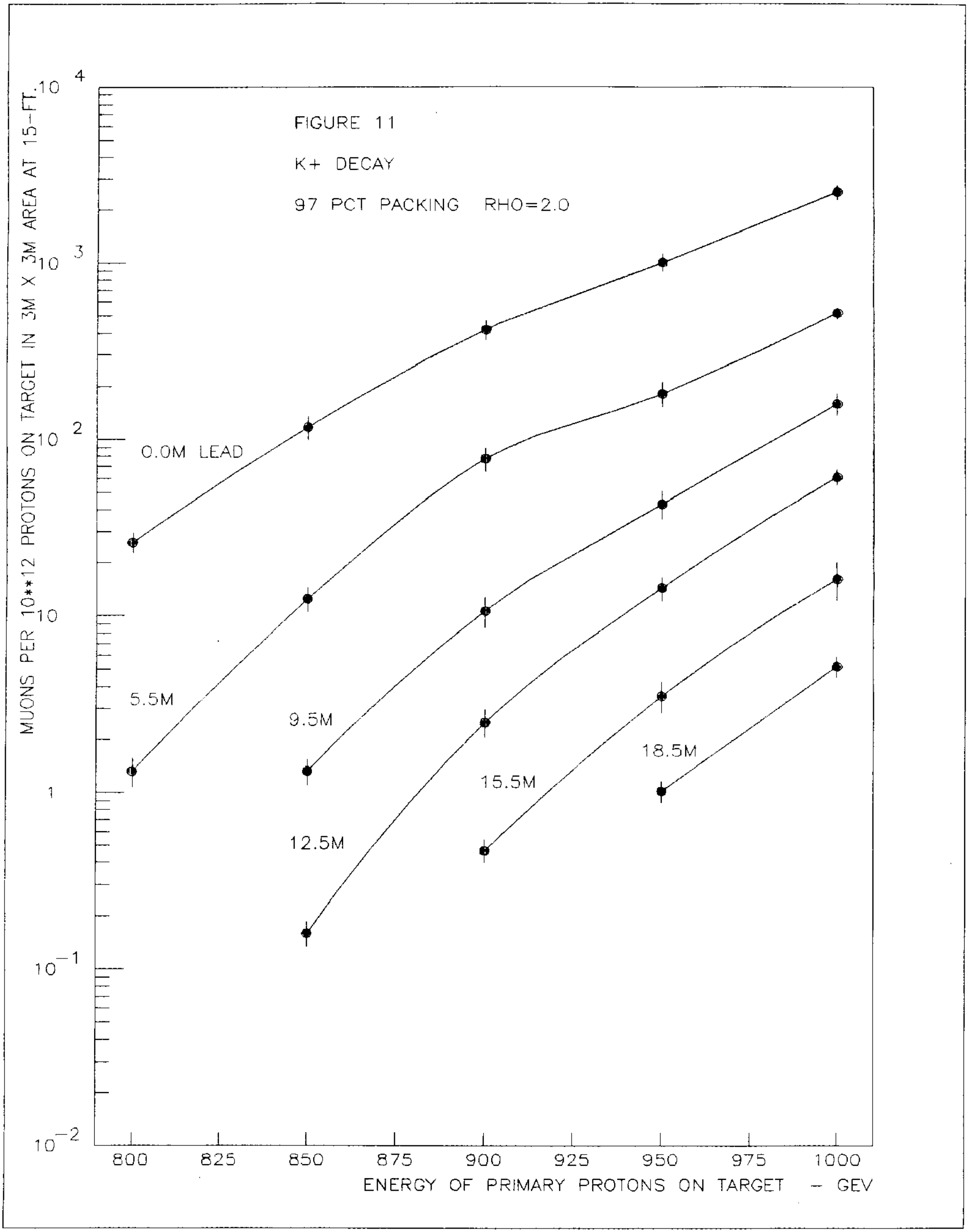

FIGURE 11
K+ DECAY
97 PCT PACKING RHO=2.0
0.0M LEAD
5.5M
9.5M
12.5M
15.5M
18.5M
MUONS PER 10**12 PROTONS ON TARGET IN 3M X 3M AREA AT 15-FT.
10^{4}
10^{3}
10^{2}
10
1
10^{-1}
10^{-2}
800
825
850
875
900
925
950
975
1000
ENERGY OF PRIMARY PROTONS ON TARGET - GEV